Large Longitudinal Spin Alignment of Excited Projectiles in Intermediate Energy Inelastic Scattering

D. E. M. Hoff,[1,*] R. J. Charity,[1] K. W. Brown,[1,†] C. D. Pruitt,[1] L. G. Sobotka,[1] T. B. Webb,[1] G. Potel,[2] B. Roeder,[3] and A. Saastamoinen[3]

[1]*Departments of Chemistry and Physics, Washington University, St. Louis, Missouri 63130, USA*

[2]*National Superconducting Cyclotron Laboratory, Michigan State University, East Lansing, Michigan 48824, USA*

[3]*Cyclotron Institute, Texas A&M University, College Station, Texas 77840, USA*

(Received 30 August 2017; published 8 December 2017)

We study the sequential breakup of $E/A = 24.0$ MeV ^{7}Li projectiles excited through inelastic interactions with C, Be, and Al target nuclei. For peripheral events that do not excite the target, we find very large spin alignment of the excited ^{7}Li projectiles longitudinal to the beam axis. This spin alignment is independent of the target used, and we propose a simple alignment mechanism that arises from an angular-momentum-excitation-energy mismatch. This mechanism is independent of the potential used for scattering and should be present in many scattering experiments.

DOI: 10.1103/PhysRevLett.119.232501

The spin polarization or alignment of exit-channel fragments produced in reactions not only provide insight into the active reaction mechanism but also enable structure studies and many applications. For example, the generation of aligned nuclear spins, the subject of the present Letter, empowers g-factor studies and thus gives insight into nuclear wave functions [1,2]. Spin-aligned molecular triplet states allow the generation of highly polarized hydrogen targets through spin transfer [3,4]. This Letter provides an example of, and an explanation for, a previously unappreciated mechanism for creating large longitudinal spin alignments in scattering experiments.

In compound [5–8], quasielastic [9], and deeply inelastic reactions [10–15], the reaction orbital angular momentum L dwarfs any intrinsic spin carried by the projectile or target. The exit-channel fragments acquire spin from the large reservoir of L and thus are characterized by transverse alignments with small projections on the beam axis. These alignments can be so strong that particles emitted from the spinning fragments exhibit a forward-backward preference as they cast off ejectiles perpendicular to the spin direction, a fact that has been used for fragment-spin determination [10,12,15]. The cases for longitudinal alignment in reactions dominated by the strong interaction are usually limited to modest modifications of the spin projections from a uniform distribution [16,17]. Large longitudinal alignment has been seen in projectile fragmentation [18], though not at the level reported in this and a related work [19]. On the other hand, at relativistic energies, Coulomb excitation will produce a large longitudinal alignment due to the Lorentz contraction of the E field [20,21].

The active mechanism for producing highly aligned inelastically scattered ^{7}Li nuclei, studied in the present Letter, does not have its origin in the Coulomb field and is independent of the reaction partner (i.e., target). The observed alignment is reproduced by a standard nuclear reaction model [22] and is a consequence of an angular-momentum-excitation-energy matching condition that requires the reaction plane to tilt when the beam energy exceeds an excitation-energy-dependent threshold. This condition is unrelated to the intrinsic spins of the fragments (not a spin-orbit effect) and is most easily visualized, and perhaps observed, in nuclei with cluster structure where the excitation changes the orbital angular momentum, ℓ, between the internal cluster pair. The origin of the matching condition generating alignment is identical to the condition, deduced by Brink, that angular-momentum conservation imposes on single-nucleon transfer reactions [23]. Namely, there is a particular kinetic-energy change, or Q-value, which matches the change in nucleon orbital momenta for optimum capture.

In our study, large spin alignment of excited ^{7}Li projectiles was observed with C, Be, and Al targets. However, this Letter will focus on the reaction with ^{12}C since it has zero spin, and the large separation between its ground and first excited state allows for selecting unexcited target nuclei in the exit channel.

The data presented in this Letter were obtained at the Texas A&M Cyclotron Institute, which provided a ^{7}Li beam at 24.0 MeV/A that impinged upon targets with thicknesses around 10 mg/cm^2. Two annular Si-CsI(Tl) telescope arrays, one looking through the hole of the other, were used to detect the pair of breakup fragments from ^{7}Li*. The upstream array used an 85-mm-diameter (3-cm-diameter hole) segmented Si (32 rings and 48 pie-shaped sectors) placed 15 cm downstream from the target. The downstream telescope used a 70-mm-diameter (22-mm-diameter hole) segmented Si (48 incomplete rings and 16 pies) and was placed 35 cm downstream from the target. Each telescope had 16 pie-shaped 2-cm-thick CsI(Tl)

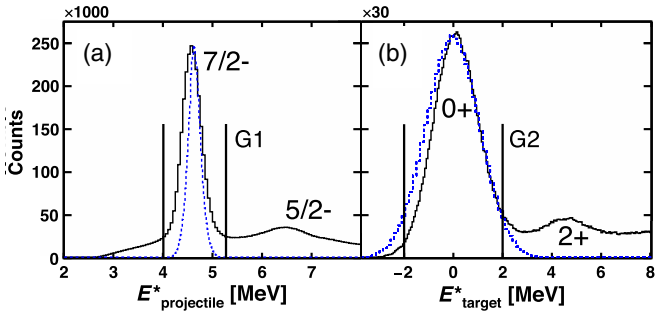

FIG. 1. Experimental distributions of excitation energy for the (a) ^{7}Li projectile and (b) the ^{12}C target.

crystals behind the Si, allowing us to measure the energy and determine the particle type of the fragments. This setup provided a polar angular range of 1.8° to 16°. Corrections to the data due to the geometric detection efficiency were determined by Monte Carlo simulations.

Note that ^{7}Li becomes unbound to $\alpha + t$ breakup at 2.467 MeV, and this is the only open channel available for the first two unbound excited states, $E^* = 4.63$ and 6.68 MeV with $J^\pi = 7/2^-$ and $5/2^-$, respectively. Both of these states are seen in the $\alpha + t$ invariant-mass reconstruction shown in Fig. 1(a). After reconstructing the ^{7}Li* momentum, 2-body kinematics was used to deduce the target's excitation energy, and the reconstructed distribution for ^{12}C is shown in Fig. 1(b). The expected resolutions from Monte Carlo simulations are shown as the blue dashed lines. This Letter only discusses events where ^{7}Li is excited to the $J^\pi = 7/2^-$ state while ^{12}C remains in its ground state. These events are selected by the gates $G1$ and $G2$ shown in Figs. 1(a) and 1(b), respectively.

Using the standard theory of angular correlations [19,24], the magnetic-substate distribution of the ^{7}Li* can be extracted from the fragment correlation angles ψ and χ. Here, ψ is the center-of-mass angle of the breakup with respect to the beam axis, and χ is the center-of-mass angle of the breakup in the plane perpendicular to the beam axis, with the x axis defined by the exit-channel scattering plane [diagrammed in Fig. 2(b)].

The efficiency-corrected angular correlations are shown in Fig. 2(a). There is a significant enhancement at $\cos(\psi) = 0$ corresponding to a preferred emission of decay fragments perpendicular to the beam axis. This means that the internal orbital angular momentum ℓ of the $\alpha + t$ pair in ^{7}Li* is preferentially aligned along the beam axis. The weights of the Legendre polynomial contributions are related to the spin density matrix of ^{7}Li*, $\rho^J_{m_1,m_2}$, for which the diagonal elements give the magnetic-substate populations [24]. The Legendre-polynomial decomposition for $\ell = 3$ is shown in Fig. 2(c). The angular correlations and decomposition are almost identical to that observed in the previous work with a secondary ^{7}Be beam and a ^{9}Be target [19]. The deduced magnetic-substrate distribution is shown in Fig. 2(d).

The level of alignment is quantified by the scalar,

$$A = \sum_{m_f} \frac{3{m_f}^2 - J(J+1)}{J(2J-1)} \rho^J_{m_f,m_f}, \tag{1}$$

where $A = 1(-1)$ corresponds to the largest possible alignment along (transverse to) the quantization axis. The magnetic-substate distribution observed corresponds to a value of $A = 0.49 \pm 0.01$. This is quite large compared to other reactions, including the longitudinal alignment of $A = 0.35(10)$ observed in the population of a high-spin isomer from projectile fragmentation [18].

Large longitudinal alignment is predicted by both a rotational (deformed) and a 3-body cluster model. However, the former does not describe the angular correlations as well as the latter. Focusing on the cluster model, the population of the $J^\pi = 7/2^-$ resonance is modeled as a direct, one-step inelastic excitation of the two-cluster $(\alpha + t)$ ^{7}Li system. The cross section is proportional to the squared modulus of the transition amplitude, or T matrix, T_{m_i,m_f}. This is calculated in the distorted-wave Born approximation (DWBA) [22] as a function of the initial, m_i, and final, m_f, projections of the ^{7}Li spin with respect to the beam axis. The distorted waves describing the relative ^{7}Li-^{12}C motion in the initial, $\chi_i(\mathbf{R})$, and final, $\chi_f(\mathbf{R})$, channels are solutions of a phenomenological central optical potential $U_{LiC}(R)$, $\mathbf{R}$ being the relative ^{7}Li-^{12}C coordinate. The ^{7}Li wave functions $\phi_{i,m_i}(\mathbf{r})$ ($J^\pi = 1/2^-$ ground state, orbital angular momentum $\ell = 1$) and $\phi_{f,m_f}(\mathbf{r})$ (excited $J^\pi = 7/2^-$ state, $\ell = 3$) are computed using a phenomenological $\alpha - t$ interaction that reproduces the ^{7}Li particle decay threshold. In order to avoid complications inherent to the treatment of the continuum, the final $J^\pi = 7/2^-$ state is modeled with a very weakly bound wave function (quasibound approximation). With these ingredients, the transition amplitude is

$$T_{m_i,m_f} = \int \chi^*_f(\mathbf{R}) \phi^*_{f,m_f}(\mathbf{r}) \Delta(R, r_{\alpha C}, r_{tC}) \times \chi_i(\mathbf{R}) \phi_{i,m_i}(\mathbf{r}) d\mathbf{r} d\mathbf{R}, \tag{2}$$

where the transition potential is

$$\Delta(R, r_{\alpha C}, r_{tC}) = U_{LiC}(R) - U_{\alpha C}(r_{\alpha C}) - U_{tC}(r_{tC}). \tag{3}$$

The α-^{12}C and t-^{12}C effective interactions, $U_{\alpha C}(r_{\alpha C})$ and $U_{tC}(r_{tC})$, are modeled by central phenomenological optical potentials depending on the corresponding distances. The optical-model parameters for the α-^{12}C and ^{7}Li-^{12}C potentials were obtained from the literature [25]. The t-^{12}C potential was extrapolated from the ^{3}He-^{12}C interaction; then, the potential parameters were constrained from a fit of the angular distributions and correlations. The $\alpha - t$ potential used was also constrained by this fit. These

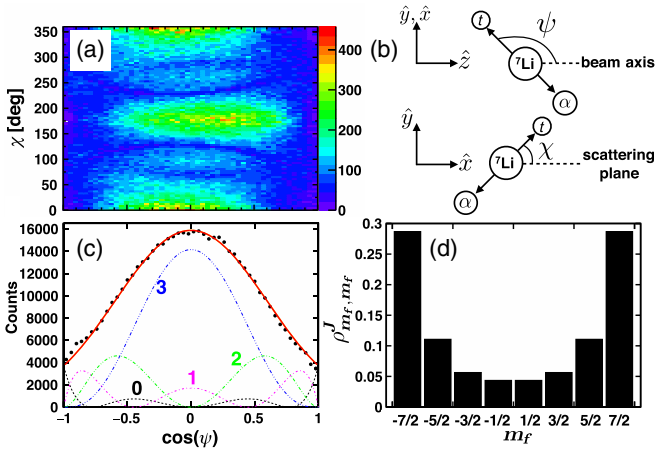

FIG. 2. (a) The efficiency-corrected angular correlations from the data for the entire angular range measured. (b) The definitions of angles ψ and χ in the rest frame of ^{7}Li. (c) The Legendre polynomial contributions from the fit to the angular correlations projected onto the cos(ψ) axis. (d) The resulting extracted magnetic-substate distribution.

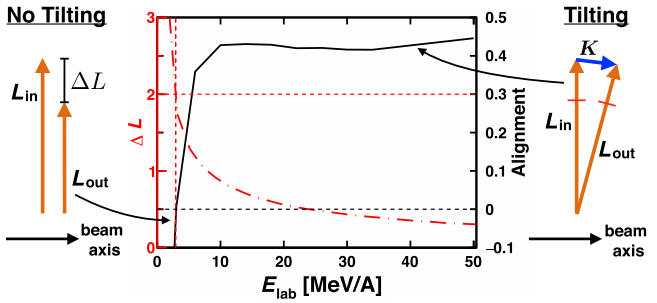

FIG. 3. Equation (4) is plotted for $E^* = 4.6$ MeV and $R = 5$ fm (red dot-dash line). The predicted alignment from the cluster-model calculations in the angular range $5° < \theta_{CM} < 15°$ as a function of beam energy is also shown (black solid line). When $\Delta L = 2\hbar$ is allowed, the alignment disappears completely ($A = 0$), corresponding to no tilting (left). For larger energies only tilting is allowed (right).

3-body fully angular-momentum-coupled cluster-model calculations were done with FRESCO [22].

The possibility that the reaction was dominated by Coulomb excitation was also considered. The cluster-model calculations predict the Coulomb excitation cross section (~0.4 mb) to be 2 orders of magnitude smaller than for nuclear excitation (~30 mb). This was corroborated by calculations for Coulomb excitation that properly take into account relativistic effects [26,27]. This is not surprising because the beam energy is modest and the targets have low Z, consistent with a previous experiment [28]. In the cluster-model calculations, the extracted alignment was not affected by removing the Coulomb potential from the interaction.

A change in the magnitude of the in-reaction-plane linear momentum corresponds to a change in the magnitude of the reaction orbital angular momentum ΔL and a center-of-mass kinetic-energy loss. For the reactions studied, the target nucleus remains in its ground state, so all of the possible center-of-mass kinetic-energy loss goes to exciting ^{7}Li. These quantities are easily related if a fixed radius R is assumed between the projectile and target during the reaction. To obtain an upper limit, it is assumed that $\mathbf{p}_{in}, \mathbf{p}_{out} \perp \mathbf{R}$, giving the Newtonian result,

$$\Delta L = R\sqrt{2\mu E_{CM}}\left(1 - \sqrt{1 - \frac{E^*}{E_{CM}}}\right), \qquad (4)$$

where μ is the reduced mass of the system and E_{CM} is the kinetic energy in the center-of-mass frame. With an excitation energy of $E^* = 4.6$ MeV, a beam energy of 24.0 MeV/A, and $R = 5$ fm (using a touching-spheres approximation), one obtains $\Delta L < 1\hbar$ for the ^{7}Li-^{12}C system. This means that a change in magnitude of the reaction orbital angular momentum cannot excite ^{7}Li to the 4.6-MeV state because $\Delta L \neq \Delta \ell = 2\hbar$. Figure 3 shows Eq. (4) plotted with the parameters relevant for the ^{7}Li + ^{12}C reaction studied (red dot-dash line).

To sidestep this mismatch, the final value of L can remain the same but tilt, giving it projection $M = \Delta m$, to allow the projectile to acquire spin. This argument for angular-momentum-excitation-energy matching suggests the observed alignment phenomenon is a threshold effect. Raising the beam energy further mismatches the angular momentum and excitation energy, but lowering it allows for nontilting of the exit-channel reaction plane. In Fig. 3, the cluster-model calculations predict the alignment will disappear, eventually changing sign, as the beam energy is lowered (black solid line). When the excitation energy can be achieved with a $2\hbar$ reduction in the reaction orbital angular momentum, tilting is no longer required to excite the state, and the alignment disappears. Diagrams for possible nontilting (left) and tilting (right) angular-momentum coupling solutions are indicated by the insets in Fig. 3.

The consequence of L tilting on the alignment of the projectile's spin can be studied by examining the properties of the T matrix. The normalized projection of the squared T matrix onto m_f (summing over m_i) provides a prediction for the final magnetic-substate distribution. Using the definition in Eq. (2), we can write the T matrix for the same incoming and outgoing L (assuming no spin-flip of the triton and employing the angular-momentum-excitation-energy matching argument; i.e., only tilting of L is allowed) as the expression

$$\begin{aligned} T^L_{m_i,m_f} \propto & \sum_{\mu_i,\mu_f,m_s} \langle \ell_i, \mu_i; 1/2, m_s | J_i, m_i \rangle \\ & \times \langle \ell_f, \mu_f; 1/2, m_s | J_f, m_f \rangle \\ & \times \int Y^{\ell_f}_{-\mu_f}(\hat{r}) Y^K_M(\hat{r}) Y^{\ell_i}_{\mu_i}(\hat{r}) d\Omega_r \\ & \times \int Y^L_{-M}(\hat{R}) Y^K_M(\hat{R}) Y^L_0(\hat{R}) d\Omega_R, \end{aligned} \qquad (5)$$

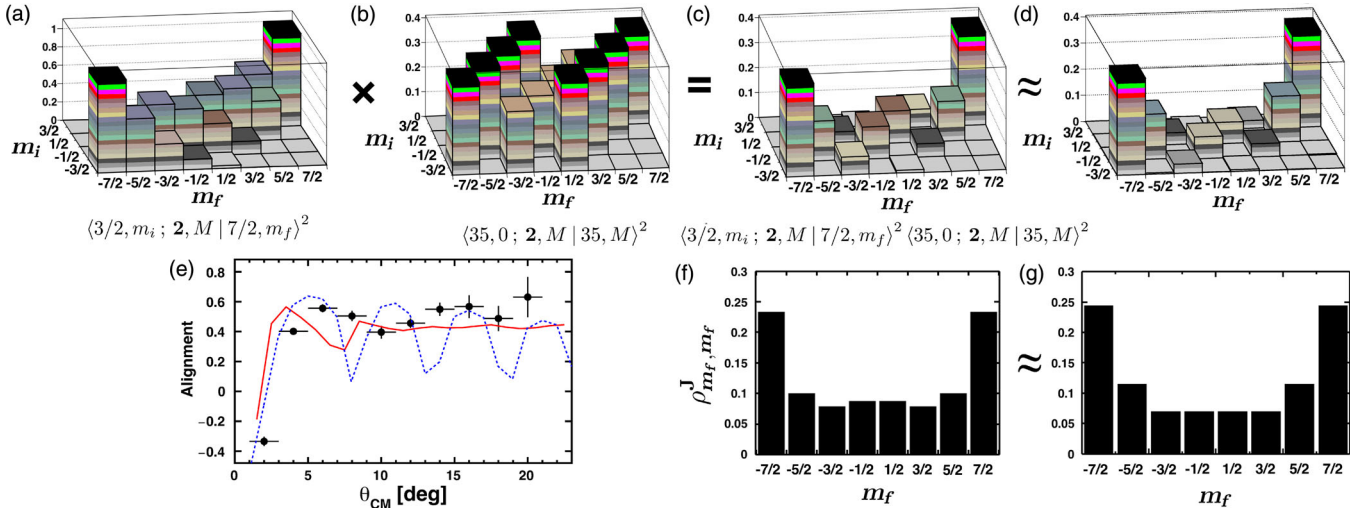

FIG. 4. The most prominent Clebsch-Gordan coefficients from angular-momentum conservation in the squared transition amplitude, $|T_{m_i,m_f}|^2$, come from (a) exciting the internal motion of the $\alpha + t$ and (b) the relative angular momentum of ^{7}Li + ^{12}C. Results are shown for grazing $L_{\text{in}} = L_{\text{out}} = L_{\text{graz}} = 35$. Panel (c) shows the multiplication of the two. (d) The squared transition amplitude calculated by the cluster model normalized to the scale of panel (c). (e) The predicted alignment, as a function of angle, from cluster-model calculations for all $\mathcal{J}$ (red solid line) and for a single $\mathcal{J} = 35.5$ (blue dashed line), as well as the data (circles). Panels (f) and (g) are normalized projections of panels (c) and (d), respectively, showing the predicted magnetic-substate distributions.

where $K = 2$ is the dominant order of the interaction. Here, K must be even because there is no change in parity between the initial and final states. The two integrals of spherical harmonics in Eq. (5) are directly proportional to Clebsch-Gordan coefficients, and the resulting T^L matrix is

$$T^L_{m_i,m_f} \propto \langle J_i, m_i; K, M | J_f, m_f\rangle \langle L, 0; K, M | L, M\rangle. \quad (6)$$

The first Clebsch-Gordan coefficient in Eq. (6) represents a change in the internal cluster orbital angular momentum of the projectile. This is coupled to a change in the relative orbital angular momentum between the projectile and target through the second (external) Clebsch-Gordan coefficient. Note that, in the external Clebsch-Gordan coefficient, the incoming relative angular momentum L has no projection along the beam axis, but after the interaction, L can have a finite spin projection, $M = \Delta m$. The values for the external Clebsch-Gordan coefficient in Eq. (6) converge for increasing L, resulting in the same alignment at higher energies. This would explain the fact that the level of alignment and angular correlations observed for 24.0 MeV/A ^{7}Li* are very similar to the previous experiment with 65.5 MeV/A ^{7}Be* [19].

The relevant squared Clebsch-Gordan coefficients in Eq. (6) are shown in Figs. 4(a) and 4(b). The internal Clebsch-Gordan coefficient prefers transitions $m_i = \pm 3/2 \rightarrow m_f = \pm 7/2$. The external Clebsch-Gordan coefficient of Eq. (6) completely suppresses $M = \pm 1$ transitions. This is due to the parity restriction that $K = 2$, so only even components of M contribute, similarly to symmetry arguments in previous studies of the polarizations perpendicular to the reaction plane in inelastic excitations [29,30]. This coefficient also enhances $M = \pm 2$ transitions relative to $M = 0$ transitions. Multiplying these together gives us the square of the T^L matrix, Fig. 4(c), which is very similar to the cluster-model calculation, Fig. 4(d). The transitions $m_i = \pm 1/2 \rightarrow m_f = \pm 5/2$ are also preferred, resulting in an increase (a "spin-up") of the ^{7}Li* spin projection along the beam axis. The similarities between the simple Clebsch-Gordan prescription and the cluster-model calculation are striking.

For a single or a few L waves, large oscillations in alignment are expected due to the high-order spherical harmonics in the wave function required for the target-projectile relative motion. This is corroborated by the cluster-model calculations of the alignment, as a function of angle for a single $\mathcal{J}$, where $\mathcal{J}$ represents the addition of L and the incoming spin of the projectile. The predicted alignment for $\mathcal{J} = 35.5$, where the calculated cross section peaks, is shown in Fig. 4(e) by the blue dashed line. When allowing mixing of the many L waves that contribute to the reaction, the oscillations in alignment with angle are washed out [solid red line in Fig. 4(e)]. This kind of interference in alignment has previously been observed [6,31] and discussed for differential cross sections [32].

Note that L-wave mixing around L_{graz} further suppresses $m_f = \pm 1/2$, as can be seen by comparing Fig. 4(f) to Fig. 4(g), though the magnitude of this effect is small. Even with this suppression, these components are still larger in the cluster-model calculation than in the data. Further study is needed to explain this additional suppression.

In summary, large spin alignment of excited ^{7}Li projectiles longitudinal to the beam axis was observed in inelastic excitations where the target remained in its ground state.

When the excitation energy is small compared to the beam energy, the reaction plane is forced to tilt in order to conserve angular momentum and energy. The relevant Clebsch-Gordan coefficients ensure that the spin projection of the excited projectile increases along the beam axis.

We believe we have uncovered a previously unappreciated alignment mechanism that was buried in standard nuclear scattering theory. This mechanism is independent of the potential used for scattering, so it should be manifest in many beam experiments. It may in fact be the active mechanism in the production of highly aligned fragments, at energies that are not highly relativistic, enabling g-factor measurements [1].

We would like to thank Carlos Bertulani for his relativistic calculation of the Coulomb excitation cross section. This work was supported by the U.S. Department of Energy, Division of Nuclear Physics under Grants No. DE-FG02-87ER-40316 and No. DE-FG02-93ER-40773.

*Corresponding author.
dhoff@go.wustl.edu
†Present Address: National Superconducting Cyclotron Laboratory, Departments of Physics and Astronomy, Michigan State University, East Lansing, MI 48824, USA.

[1] P. F. Mantica, A. E. Stuchbery, D. E. Groh, J. I. Prisciandaro, and M. P. Robinson, Phys. Rev. C **63**, 034312 (2001).
[2] Y. Utsuno, Phys. Rev. C **70**, 011303 (2004).
[3] T. Wakui, M. Hatano, H. Sakai, T. Uesaka, and A. Tamii, Nucl. Instrum. Methods Phys. Res., Sect. A **550**, 521 (2005).
[4] D. J. Sloop, H. Yu, T. Lin, and S. I. Weissman, J. Chem. Phys. **75**, 3746 (1981).
[5] Z. Majka, D. G. Sarantites, L. G. Sobotka, K. Honkanen, E. L. Dines, L. A. Adler, L. Ze, M. L. Halbert, J. R. Beene, D. C. Hensley *et al.*, Phys. Rev. Lett. **58**, 322 (1987).
[6] A. H. Wuosmaa, R. W. Zurmühle, P. H. Kutt, S. F. Pate, S. Saini, M. L. Halbert, and D. C. Hensley, Phys. Rev. Lett. **58**, 1312 (1987).
[7] F. A. Dilmanian, D. G. Sarantites, M. Jääskeläinen, H. Puchta, R. Woodward, J. R. Beene, D. C. Hensley, M. L. Halbert, R. Novotny, L. Adler *et al.*, Phys. Rev. Lett. **49**, 1909 (1982).
[8] N. G. Nicolis, D. G. Sarantites, L. A. Adler, F. A. Dilmanian, K. Honkanen, Z. Majka, L. G. Sobotka, Z. Li, T. M. Semkow, J. R. Beene *et al.*, Phys. Rev. C **41**, 2118 (1990).
[9] R. Puigh, P. Dyer, R. Vandenbosch, T. Thomas, L. Nunnelley, and M. Zisman, Phys. Lett. **86B**, 24 (1979).
[10] D. Fick, Annu. Rev. Nucl. Part. Sci. **31**, 53 (1981).
[11] G. J. Wozniak, R. J. McDonald, A. J. Pacheco, C. C. Hsu, D. J. Morrissey, L. G. Sobotka, L. G. Moretto, S. Shih, C. Schück, R. M. Diamond *et al.*, Phys. Rev. Lett. **45**, 1081 (1980).
[12] L. G. Sobotka, C. C. Hsu, G. J. Wozniak, D. J. Morrissey, and L. G. Moretto, Nucl. Phys. **A371**, 510 (1981).
[13] D. J. Morrissey, G. J. Wozniak, L. G. Sobotka, R. J. McDonald, A. J. Pacheco, and L. G. Moretto, Nucl. Phys. **A442**, 578 (1985).
[14] P. Dyer, R. Puigh, R. Vandenbosch, T. Thomas, M. Zisman, and L. Nunnelley, Nucl. Phys. **A322**, 205 (1979).
[15] D. Morrissey, G. Wozniak, L. Sobotka, A. Pacheco, R. McDonald, C. Hsu, and L. Moretto, Nucl. Phys. **A389**, 120 (1982).
[16] Y. Ichikawa, H. Ueno, Y. Ishii, T. Furukawa, A. Yoshimi, D. Kameda, H. Watanabe, N. Aoi, K. Asahi, D. L. Balabanski *et al.*, Nat. Phys. **8**, 918 (2012).
[17] M. Kmiecik, A. Maj, J. Gerl, G. Neyens, L. Atanasova, D. Balabanski, F. Becker, P. Bednarczyk, G. Benzoni, N. Blasi *et al.*, Eur. Phys. J. A **45**, 153 (2010).
[18] W.-D. Schmidt-Ott, K. Asahi, Y. Fujita, H. Geissel, K.-D. Gross, T. Hild, H. Irnich, M. Ishihara, K. Krumbholz, V. Kunze *et al.*, Z. Phys. A **350**, 215 (1994).
[19] R. J. Charity, J. M. Elson, J. Manfredi, R. Shane, L. G. Sobotka, Z. Chajecki, D. Coupland, H. Iwasaki, M. Kilburn, J. Lee *et al.*, Phys. Rev. C **91**, 024610 (2015).
[20] J. Ritman, F.-D. Berg, W. Kühn, V. Metag, R. Novotny, M. Notheisen, P. Paul, M. Pfeiffer, O. Schwalb, H. Löhner *et al.*, Phys. Rev. Lett. **70**, 533 (1993).
[21] C. A. Bertulani and G. Baur, Phys. Rep. **163**, 299 (1988).
[22] I. J. Thompson, Comput. Phys. Rep. **7**, 167 (1988).
[23] D. Brink, Phys. Lett. **40B**, 37 (1972).
[24] G. R. Satchler, *Direct Nuclear Reactions* (Oxford University Press, Oxford, 1983).
[25] C. M. Perey and F. G. Perey, At. Data Nucl. Data Tables **17**, 1 (1976).
[26] C. A. Bertulani, A. E. Stuchbery, T. J. Mertzimekis, and A. D. Davies, Phys. Rev. C **68**, 044609 (2003).
[27] C. A. Bertulani (private communication).
[28] J. E. Mason, S. B. Gazes, R. B. Roberts, and S. G. Teichmann, Phys. Rev. C **45**, 2870 (1992).
[29] A. Bohr, Nucl. Phys. **10**, 486 (1959).
[30] F. Schmidt, R. E. Brown, J. Gerhart, and W. A. Kolasinski, Nucl. Phys. **52**, 353 (1964).
[31] P. Wust, W. von Oertzen, H. Ossenbrink, H. Lettau, H. G. Bohlen, W. Saathoff, and C. A. Wiedner, Z. Phys. A **291**, 151 (1979).
[32] N. Austern, *Direct Nuclear Reaction Theories*, Interscience Monographs and Texts in Physics and Astronomy (Wiley-Interscience, New York, 1970).